COMMUN. MATH. SCI.
Vol. 6, No. 2, pp. 385–396

A REDUCED MODEL FOR INTERNAL WAVES INTERACTING WITH TOPOGRAPHY AT INTERMEDIATE DEPTH*

AILÍN RUIZ DE ZÁRATE† AND ANDRÉ NACHBIN‡

Abstract. A reduced strongly nonlinear model is derived for the evolution of one-dimensional internal waves over an arbitrary bottom topography. Two layers containing inviscid, immiscible, irrotational fluids of different densities are defined. The upper layer is shallow compared with the characteristic wavelength at the interface, while the bottom region's depth is comparable to the wavelength. The nonlinear evolution equations obtained are in terms of the internal wave elevation and the mean upper-velocity for the configuration described. The system is a generalization of the one proposed by Choi and Camassa for the flat bottom case in the same physical settings. Due to the presence of a topography a variable coefficient system of partial differential equations arises. These Boussinesq-type equations contain the Intermediate Long Wave (ILW) equation and the Benjamin-Ono (BO) equation when restricted to the unidirectional propagation regime. We intend to use this model to study the interaction of waves with the bottom profile. The dynamics include wave scattering, dispersion and attenuation, among other phenomena.

Key words. internal waves, inhomogeneous media, asymptotic theory

AMS subject classifications. 76B55, 76B15, 76B07, 35Q35

1. Introduction

Modeling internal waves is of great interest in the study of ocean and atmosphere dynamics. Internal ocean waves, for example, appear when salt concentration and differences in temperature generate stratification. They can interact with the bottom topography and submerged structures as well as with surface waves. In particular, in oil recovery in deep ocean waters, internal waves can affect offshore operations and submerged structures. Another example in the context of atmosphere dynamics is the effect of the form drag of the topography (such as an urban area) which is of importance in the study of pollution dispersion. The understanding of the impact of the orography as well as smaller topographic features on the atmosphere can lead to a significant improvement in weather forecasting. Accurate reduced models are a first step in producing efficient computational methods in engineering problems in oceanography and meteorology. This was the goal in [24, 1]. Hence, in deriving the present reduced model we also have in mind obtaining efficient numerical methods for internal waves interacting with topographies. We are currently investigating related numerical schemes.

To describe this nonlinear wave phenomenon in deep water there are several bidirectional models containing the Intermediate Long Wave (ILW) equation and the Benjamin-Ono (BO) equation, starting from works such as [2, 8, 26, 16, 18] to more recent papers such as [20, 5, 6, 7, 15]. These models consider flat or slowly varying bottom topography. In this paper the model of Choi and Camassa is generalized to the case of an arbitrary bottom topography by using the conformal mapping technique

*Received: May 29, 2007; accepted (in revised version): March 16, 2008. Communicated by Paul Milewski.

†Instituto de Matemática Pura e Aplicada, Estrada Dona Castorina 110, Jardim Botânico, Rio de Janeiro, RJ, CEP 22460-320, Brazil (ailin@impa.br). The author was supported by an ANP/PRH-32 scholarship.

‡Instituto de Matemática Pura e Aplicada, Estrada Dona Castorina 110, Jardim Botânico, Rio de Janeiro, RJ, CEP 22460-320, Brazil (nachbin@impa.br). This work was supported by CNPq/Brazil under Grant 300368/96-8.

described in [24]. We obtain a strongly nonlinear long-wave model like Choi and Camassa's which is able to describe large amplitude internal solitary waves. Two fluid layers are constrained to a region limited by a horizontal rigid lid at the top and an arbitrary topography at the bottom, as described in Figure 2.1. The upper layer is shallow compared with the characteristic wavelength at the fluid interface, while the lower region is deeper. The nonlinear fluid equations obtained describe the evolution of the internal wave elevation together with the mean water velocity for the upper layer. These Boussinesq-type equations contain the ILW equation and the BO equation when considering the unidirectional propagation regime. We intend to use this model to study the interaction of waves with the bottom profile, including topics such as wave scattering, dispersion and attenuation, among others.

The paper is organized as follows. In Section 2 the physical setting is presented. The corresponding mathematical models are given for both layers. The upper layer is averaged in the vertical direction and coupled to the lower layer. The continuity of pressure at the interface establishes a connection between both layers. Through this condition topography information is transmitted to the upper layer. In Section 3 a variable coefficient ILW equation and the BO equation are obtained from the reduced model restricted to the unidirectional propagation regime. Technical justifications for the manipulations done in Section 3 are provided in Appendix A.

2. Derivation of the reduced equations

We start with a two-fluid configuration. The coordinate system is positioned at the undisturbed interface between layers. The displacement of the interface is denoted by $\eta(x,t)$ and we may assume that initially it has compact support. See Figure 2.1. The density of each inviscid, immiscible, irrotational fluid is ρ_1 for the upper fluid and ρ_2 for the lower fluid. For a stable stratification, let $\rho_2>\rho_1$. Similarly, (u_i,w_i) denotes the velocity components and p_i the pressure, where $i=1,2$. The upper layer is assumed to have a characteristic thickness of h_1, much smaller than the characteristic wavelength L at the interface. Hence, the upper layer will be in the shallow water regime. At the lower layer the irregular bottom is described by $z=h_2(h(x/l)-1)$, $h<1$. The function h can be discontinuous or even multivalued. See for example Figure 2.1 where a polygonal shaped topography is sketched. We can assume h has compact support so that the roughness is confined to a finite interval. Moreover the characteristic depth for the lower layer h_2 is comparable with the characteristic wavelength L, hence characterizing an intermediate depth regime. When a rapidly varying bottom is taken into account, the horizontal length scale for bottom irregularities l is such that $h_1<l\ll L$. On the other hand, in the slowly varying bottom case we define $\varepsilon=L/l\ll 1$.

The corresponding Euler equations are

$$\begin{aligned} u_{ix}+w_{iz}&=0,\\ u_{it}+u_iu_{ix}+w_iu_{iz}&=-p_{ix}/\rho_i,\\ w_{it}+u_iw_{ix}+w_iw_{iz}&=-p_{iz}/\rho_i-g, \end{aligned}$$

for $i=1,2$. Subscripts x, z and t stand for partial derivatives with respect to spatial coordinates and time. The continuity condition at the interface $z=\eta(x,t)$ requires that $\eta_t+u_i\eta_x=w_i$ and $p_1=p_2$, namely, a kinematic condition for the material curve together with no pressure jumps. At the top we impose a rigid lid condition $w_1(x,h_1,t)=0$, commonly used in ocean and atmospheric models, while at the irregular impermeable bottom $-h_2h'(x/l)u_2/l+w_2=0$.

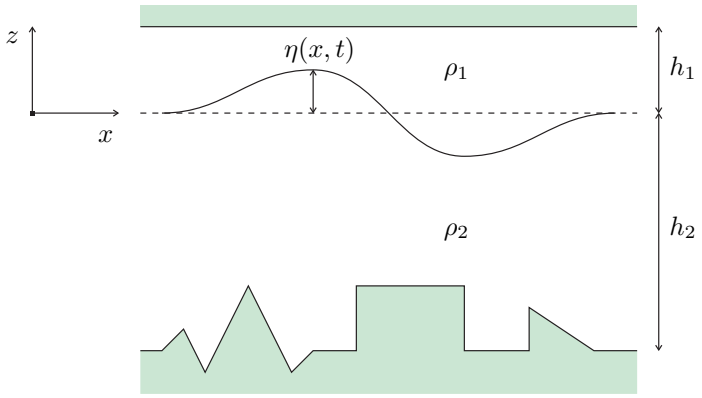

FIG. 2.1. *Two-fluid system configuration.*

Introducing the nondimensional dispersion parameter $\beta=(h_1/L)^2$, it follows that $O\left(\sqrt{\beta}\right)=O(h_1/L)\ll 1$. From the conservation of mass equation with $i=1$ we have $w_1/u_1=O(h_1/L)=O\left(\sqrt{\beta}\right)$.

Let $U_0=\sqrt{gh_1}$ be the characteristic shallow layer speed. Now let the physical variables regarding the upper layer be nondimensionalized as follows:

$$x=L\tilde{x}, \qquad z=h_1\tilde{z}, \qquad t=\frac{L}{U_0}\tilde{t}, \qquad \eta=h_1\tilde{\eta},$$
$$p_1=(\rho_1 U_0^2)\tilde{p_1}, \qquad u_1=U_0\tilde{u}_1, \qquad w_1=\sqrt{\beta}U_0\tilde{w}_1.$$

In a weakly nonlinear theory, η is usually scaled by a small characteristic amplitude a such that $a/h_1\ll 1$. Notice that here η is of the same order as the layer's depth. This will lead to a strongly nonlinear model.

2.1. Reducing the upper layer dynamics to the interface. The nondimensional equations for the upper layer (the tilde has been removed) are:

$$u_{1x}+w_{1z}=0, \tag{2.1}$$
$$u_{1t}+u_1u_{1x}+w_1u_{1z}=-p_{1x}, \tag{2.2}$$
$$\beta(w_{1t}+u_1w_{1x}+w_1w_{1z})=-p_{1z}-1. \tag{2.3}$$

The boundary conditions are

$$\eta_t+u_1\eta_x=w_1 \quad \text{and} \quad p_1=p_2 \quad \text{at} \quad z=\eta(x,t), \tag{2.4}$$
$$w_1(x,1,t)=0. \tag{2.5}$$

Consider the following definition for a *mean-layer quantity* $\overline{f}$:

$$\overline{f}(x,t)=\frac{1}{1-\eta}\int_{\eta}^{1} f(x,z,t)\,dz.$$

Through averaging, the two-dimensional (2D) Euler equations (2.1, 2.2, 2.3) and boundary conditions (2.4, 2.5) can be reduced to the following one-dimensional (1D)

system along the interface:

$$-\eta_{1t} = (\eta_1 \overline{u_1})_x, \tag{2.6}$$

$$(\eta_1 \overline{u_1})_t + \left(\eta_1 \overline{u_1^2}\right)_x = -\eta_1 \overline{p_{1x}}, \tag{2.7}$$

where $\eta_1 = 1-\eta$.

As pointed out in [7], the system of equations (2.6)–(2.7) was already considered in [27, 4] for surface waves. In reducing (averaging) the 2D Euler equations to the 1D system above, no approximations have yet been made. Nevertheless, the quantities $\overline{u_1 u_1}$ and $\overline{p_{1x}}$ prevent the closure of the system (2.6)–(2.7). In [7], these quantities were expressed in terms of η and $\overline{u_1}$ up to a certain order in the dispersion parameter β. Some steps are repeated here for convenience. We start by approximating $\overline{p_{1x}}$ and then proceed to do the same for $\overline{u_1 u_1}$.

The vertical momentum equation (2.3) suggests an expansion in powers of β as

$$f(x,z,t) = f^{(0)} + \beta f^{(1)} + O(\beta^2) \tag{2.8}$$

for any of the functions u_1, w_1, p_1. From equation (2.3) we get that $p_{1z} = -1 + O(\beta)$. Integration from η to z together with the pressure continuity across the interface gives

$$p_1(x,z,t) = p_2(x,\eta,t) - (z-\eta) + O(\beta). \tag{2.9}$$

Pressure $p_2(x,\eta,t)$ should be nondimensionalized in the same fashion as p_1, that is, $p_2 = \rho_1 U_0^2 \tilde{p}_2$.

From now on the pressure at the interface will be denoted as $P(x,t) = p_2\big(x,\eta(x,t),t\big)$. Then, from equation (2.9) we have

$$\overline{p_{1x}} = P_x + \eta_x + O(\beta). \tag{2.10}$$

An approximation for P_x will be obtained below by using Euler equations for the intermediate depth lower layer.

To approximate the mean squared horizontal velocity to leading order, notice that the irrotational condition in nondimensional variables is $u_{1z} = \beta w_{1x}$. Hence, $({u_1}^{(0)})_z = 0$, and, as expected, for shallow water flows $u_1^{(0)}$ is independent from z. Therefore,

$$\eta_1 \overline{u_1 u_1} = \eta_1 \overline{u_1}\,\overline{u_1} + O(\beta). \tag{2.11}$$

Using equation (2.11) and equation (2.6), equation (2.7) becomes $\eta_1 \overline{u_1}_t + \eta_1 \overline{u_1}\,\overline{u_1}_x = -\eta_1 \overline{p_{1x}} + O(\beta)$. After substitution of equation (2.10), the following set of approximate equations are obtained for the upper layer:

$$-\eta_t + \big((1-\eta)\overline{u_1}\big)_x = 0, \tag{2.12}$$

$$\overline{u_1}_t + \overline{u_1}\,\overline{u_1}_x = -\eta_x - P_x + O(\beta). \tag{2.13}$$

Now it remains to find an expression for P_x in order to close the system and also to establish a connection with the lower intermediate depth layer.

2.2. Connecting the upper and lower layers. As mentioned above, the coupling of the upper and lower layers is done through the pressure term. In order to get an approximation for P_x from the Euler equations at the lower fluid layer,

observe that the intermediate depth regime implies that $h_2/L = O(1)$. Hence, the scaling $w_2/u_2 = O(h_2/L) = O(1)$ is valid as a consequence of the conservation of mass equation. At the interface, from the continuity of vertical velocities together with the relations above, we have that $w_2/u_1 = O\left(\sqrt{\beta}\right)$ and $u_2/u_1 = O\left(\sqrt{\beta}\right)$. These relations induce the following nondimensional variables (with a tilde) for the lower region:

$$x = L\tilde{x}, \qquad z = L\tilde{z}, \qquad t = \frac{L}{U_0}\tilde{t}, \qquad \eta = h_1\tilde{\eta},$$
$$p_2 = (\rho_1 U_0^2)\tilde{p}_2, \qquad u_2 = \sqrt{\beta}U_0\tilde{u}_2, \qquad w_2 = \sqrt{\beta}U_0\tilde{w}_2.$$

This naturally suggests that we introduce the velocity potential $\phi = \sqrt{\beta}U_0 L\tilde{\phi}$.

In these nondimensional variables, the Bernoulli law at the interface reads

$$\sqrt{\beta}\phi_t + \frac{\beta}{2}\left(\phi_x^2 + \phi_z^2\right) + \eta + \frac{\rho_1}{\rho_2}P = \mathcal{C}(t),$$

where the tilde has been ignored. $\mathcal{C}(t)$ is an arbitrary function of time. Then, up to order β, P_x is given as

$$P_x = -\frac{\rho_2}{\rho_1}\left(\eta_x + \sqrt{\beta}\phi_t(x, \sqrt{\beta}\eta, t)_x\right) + O(\beta), \tag{2.14}$$

where ϕ satisfies the following free surface Neumann problem,

$$\begin{cases} \phi_{xx} + \phi_{zz} = 0 & \text{on } -h_2/L + h_2 h(Lx/l)/L \le z \le \sqrt{\beta}\eta(x,t), \\ \phi_z = \eta_t + \sqrt{\beta}\eta_x\phi_x & \text{at } z = \sqrt{\beta}\eta(x,t), \\ -(h_2/l)h'(Lx/l)\phi_x + \phi_z = 0 & \text{at } z = -h_2/L + h_2 h(Lx/l)/L. \end{cases} \tag{2.15}$$

Furthermore, expanding in z gives

$$P_x = -\frac{\rho_2}{\rho_1}\left(\eta_x + \sqrt{\beta}\phi_{tx}(x,0,t)\right) + O(\beta). \tag{2.16}$$

As in the flat bottom case [7], it is sufficient to find ϕ_{tx} at $z = 0$ in order to approximate P_x at the interface. Therefore, we consider the linear problem

$$\begin{cases} \phi_{xx} + \phi_{zz} = 0 & \text{on } -h_2/L + h_2 h(Lx/l)/L \le z \le 0, \\ \phi_z = \eta_t & \text{at } z = 0, \\ -(h_2/l)h'(Lx/l)\phi_x + \phi_z = 0 & \text{at } z = -h_2/L + h_2 h(Lx/l)/L. \end{cases} \tag{2.17}$$

A conformal mapping is performed between the flat strip $\zeta \in \left[-\frac{h_2}{L}, 0\right]$ and the lower layer at rest. See Figure 2.2.

Then problem (2.17) in conformal coordinates becomes

$$\begin{cases} \phi_{\xi\xi} + \phi_{\zeta\zeta} = 0 & \text{on } -h_2/L \le \zeta \le 0, \\ \phi_\zeta(\xi, 0, t) = M(\xi)\eta_t\left(\mathrm{x}(\xi,0), t\right) & \text{at } \zeta = 0, \\ \phi_\zeta = 0 & \text{at } \zeta = -h_2/L, \end{cases} \tag{2.18}$$

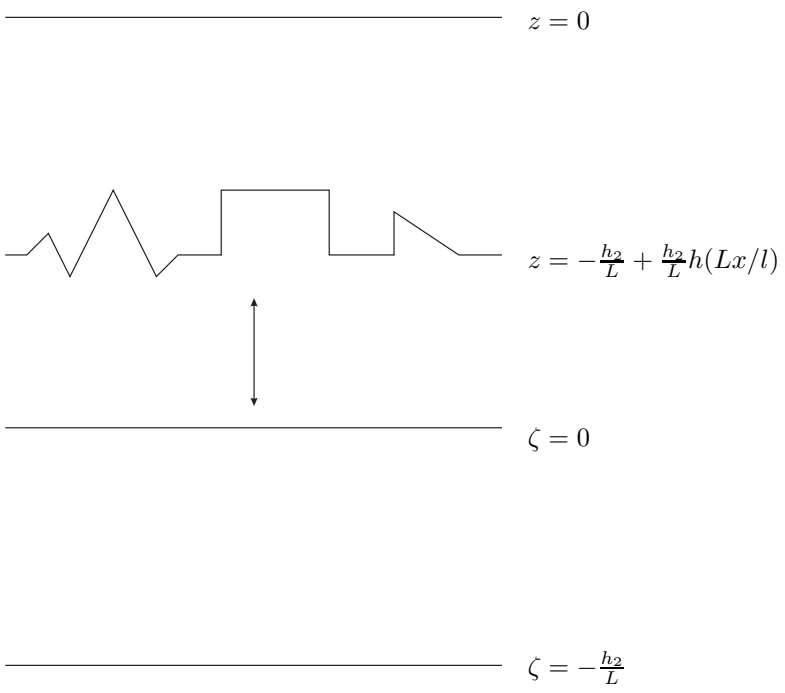

FIG. 2.2. *Conformal mapping,* $(x,z) = \big(\mathrm{x}(\xi,\zeta), z(\xi,\zeta)\big)$.

where the Neumann condition at the undisturbed interface now has a variable coefficient $M(\xi) = \mathrm{z}_\zeta(\xi,0)$. The new coefficient is the nonzero element of the Jacobian evaluated at the undisturbed interface. As shown in [24], its exact expression is

$$M(\xi_0) = 1 - \frac{\pi}{4}\frac{L}{h_2}\int_{-\infty}^{\infty} \frac{h\big(L\mathrm{x}(\xi,-h_2/L)/l\big)}{\cosh^2\Big(\frac{\pi L}{2h_2}(\xi-\xi_0)\Big)}\,d\xi.$$

Moreover, the Jacobian evaluated along the undisturbed interface is an analytic function. Hence a highly complex boundary profile has been converted into a smooth coefficient.

Since a conformal mapping was used in the coordinate transformation and $\mathrm{z}_\xi(\xi,0) = 0$, it is guaranteed that $\mathrm{z}_\zeta(\xi,0) = \mathrm{x}_\xi(\xi,0)$ is different from zero. The horizontal velocity is recovered as $\phi_x(x,0,t) = \phi_\xi(\xi,0,t)/M(\xi)$.

Notice that the terrain-following velocity component $\phi_\xi(\xi,0,t)$ is a tangential derivative on the boundary for problem (2.18). Hence it can be obtained as the Hilbert transform on the strip (see [17]) applied to the Neumann data. Namely,

$$\phi_\xi(\xi,0,t) = \mathcal{T}\Big[M(\tilde{\xi})\eta_t\big(\mathrm{x}(\tilde{\xi},0),t\big)\Big](\xi),$$

where

$$\mathcal{T}[f](\xi) = \frac{1}{2h}\fint f(\tilde{\xi})\coth\Big(\frac{\pi}{2h}(\tilde{\xi}-\xi)\Big)\,d\tilde{\xi} \tag{2.19}$$

is the Hilbert transform on the strip of height h. In this case, $h = h_2/L$. The singular integral must be interpreted as a Cauchy principal value. The solution of the

two-dimensional linear problem below the interface has been collapsed onto a one-dimensional singular integral without any approximation. This result is then used in (2.16) by noting that ϕ_{tx} is obtained after taking the time derivative of problem (2.17).

Substituting the expression for P_x in the upper layer averaged equations gives

$$\begin{cases} \eta_t - \left[(1-\eta)\overline{u_1}\right]_x = 0, \\ \overline{u_1}_t + \overline{u_1}\,\overline{u_1}_x + \left(1-\dfrac{\rho_2}{\rho_1}\right)\eta_x = \sqrt{\beta}\dfrac{\rho_2}{\rho_1}\dfrac{1}{M(\xi)}\mathcal{T}\left[M(\cdot)\eta_{tt}\big(\mathrm{x}(\cdot,0),t\big)\right] + O(\beta), \end{cases} \tag{2.20}$$

where the dot indicates the variable on which the operator $\mathcal{T}$ is applied. It remains to make a few manipulations with this set of equations: eliminate the second order derivative in time and write all spatial derivatives in ξ. Notice that the first equation is exact. Hence $\eta_{tt} = \big((1-\eta)\overline{u_1}\big)_{xt}$, and we substitute this relation in the right-hand side of the second equation.

The Hilbert transform is in curvilinear coordinates. Recall that every x-derivative is equal to a ξ-derivative divided by the Jacobian $M(\xi)$. Therefore, in terrain-following coordinates, system (2.20) reads as

$$\begin{cases} \eta_t - \dfrac{1}{M(\xi)}\left[(1-\eta)\overline{u_1}\right]_\xi = 0, \\ \overline{u_1}_t + \dfrac{1}{M(\xi)}\overline{u_1}\,\overline{u_1}_\xi + \dfrac{1}{M(\xi)}\left(1-\dfrac{\rho_2}{\rho_1}\right)\eta_\xi = \sqrt{\beta}\dfrac{\rho_2}{\rho_1}\dfrac{1}{M(\xi)}\mathcal{T}\left[\big((1-\eta)\overline{u_1}\big)_{\xi t}\right]. \end{cases} \tag{2.21}$$

This is a variable-coefficient Boussinesq-type system depending on $M(\xi)$ which has information from the topography. As will be shown below, this is a dispersive model, where the dispersion term comes in through the Hilbert transform. The model is strongly nonlinear, since up to this point the wave amplitude was not considered to be small. If the bottom is flat, $M(\xi)=1$ and we obtain the same system derived in [7]. Efficient computational methods can be produced for this accurate reduced model which governs, to leading order, a complex two-dimensional problem. For the flat-bottom version of system (2.21), Choi and Camassa [7] used a pseudospectral method in space. They perform the evolution in time for η and V, where $V = \overline{u_1} - \sqrt{\beta}\,\frac{\rho_2}{\rho_1}\mathcal{T}\left[\big((1-\eta)\overline{u_1}\big)_\xi\right]$. The time evolution was performed by a fourth order Runge-Kutta integration scheme. To recover $\overline{u_1}$ after each time step, an algebraic system was solved involving the spectral differentiation matrix for the spatial derivative (namely via a DFT procedure) and the convolution matrix for the operator $\mathcal{T}$. Since our model (2.21) differs only through a variable (time independent) coefficient, this numerical formulation applies. The Jacobian $M(\xi)$ is computed using Driscoll's package [9]. Results regarding these computational methods will be published elsewhere in the near future. We intend to perform experiments over random topographies as those presented in [13, 22, 10, 25, 14] regarding the apparent diffusion and time-reversal refocusing of waves [23, 12, 10, 11].

When the lower depth tends to infinity ($h_2 \to \infty$) the limit for this model is the same as obtained in [7], ($M(\xi)\to 1$ and $\mathrm{x}(\tilde{\xi},0)\to\tilde{\xi}$). In this infinite lower layer regime, system (2.20) becomes

$$\begin{cases} \eta_t - \left[(1-\eta)\overline{u_1}\right]_x = 0, \\ \overline{u_1}_t + \overline{u_1}\,\overline{u_1}_x + \left(1-\dfrac{\rho_2}{\rho_1}\right)\eta_x = \sqrt{\beta}\dfrac{\rho_2}{\rho_1}\mathcal{H}\left[\big((1-\eta)\overline{u_1}\big)_{xt}\right], \end{cases} \tag{2.22}$$

where $\mathcal{H}$ is the usual Hilbert transform defined as

$$\mathcal{H}[f](x) = \frac{1}{\pi} \int \frac{f(\tilde{x})}{\tilde{x} - x}\, d\tilde{x}.$$

Below we will comment on how the regularized Benjamin–Ono equation arises from the unidirectional propagation regime of the above system.

The dispersion relation for the intermediate depth model ($M(\xi) = 1$) is [7]:

$$\omega^2 = \frac{\left(\frac{\rho_2}{\rho_1} - 1\right) k^2}{1 + \frac{\rho_2}{\rho_1} k \sqrt{\beta} \coth\left(\frac{k h_2}{L}\right)}. \tag{2.23}$$

We note that full dispersion is retained in the lower layer when compared to the linearized Euler equations [19]. Observe also that $\omega^2/k^2 \to 0$ as $k \to \infty$, leading to bounded phase velocities as k becomes large.

3. Unidirectional propagation regime

For a slowly varying topography and weakly nonlinear waves, our model reduces to a single unidirectional ILW equation with variable coefficients.

Consider again system (2.20), but now with

$$M(\xi_0) = 1 - \frac{\pi}{4} \frac{L}{h_2} \int_{-\infty}^{\infty} \frac{h\left(\varepsilon \mathrm{x}(\xi, -h_2/L)\right)}{\cosh^2\left(\frac{\pi L}{2h_2}(\xi - \xi_0)\right)}\, d\xi,$$

due to a slowly varying bottom topography $z = -h_2/L + (h_2/L) h(\varepsilon x)$, with $\varepsilon \ll 1$. The restriction to a slowly varying topography is consistent with the objective of the present section, which is to assume that there will be no reflection nor any backward propagation.

To study the weakly nonlinear regime, introduce the nonlinearity parameter $\alpha = a/h_1 = O\left(\sqrt{\beta}\right)$, where a is the typical wave amplitude. Furthermore we rescale the nondimensional variables by setting $\eta = \alpha \eta^*$, $\overline{u_1} = \alpha c_0 \overline{u_1}^*$ and $t = t^*/c_0$, where $c_0^2 = (\rho_2/\rho_1 - 1)$. Depending on the root c_0 chosen, we have a right- or left-going wave.

Then, dropping the asterisks, we have

$$\begin{cases} \eta_t - \left[(1 - \alpha\eta)\overline{u_1}\right]_x = 0, \\ \overline{u_1}_t + \alpha \overline{u_1}\, \overline{u_1}_x - \eta_x = \sqrt{\beta} \dfrac{\rho_2}{\rho_1} \dfrac{1}{M(\xi)} \mathcal{T}\left[M(\tilde{\xi}) \overline{u_1}_{xt}\right] + O\left(\beta, \alpha\sqrt{\beta}\right). \end{cases} \tag{3.1}$$

Now we generalize the relation between η and $\overline{u_1}$ considered in [7]. In our variable coefficient model we consider

$$\eta = A_1 \overline{u_1} + \alpha A_2 \overline{u_1}^2 + \sqrt{\beta} A_3 \frac{1}{M(\xi)} \mathcal{T}\left[M(\tilde{\xi}) \overline{u_1}_t\right] + O\left(\alpha^2, \beta, \alpha\sqrt{\beta}\right), \tag{3.2}$$

with coefficients A_i, $i = 1, \ldots, 3$ to be determined. Substituting equation (3.2) into equations (3.1), two equations for $\overline{u_1}$ are obtained:

$$\begin{aligned} 0 = {} & A_1 \overline{u_1}_t - \overline{u_1}_x + \alpha A_2 \left(\overline{u_1}^2\right)_t + \alpha A_1 \left(\overline{u_1}^2\right)_x \\ & + \frac{\sqrt{\beta} A_3}{M(\xi)} \mathcal{T}\left[M(\tilde{\xi}) \overline{u_1}_{tt}\right] + O\left(\alpha^2, \beta, \alpha\sqrt{\beta}\right), \end{aligned} \tag{3.3}$$

$$0=\overline{u_1}_t-A_1\overline{u_1}_x+\alpha(1/2-A_2)\left(\overline{u_1}^2\right)_x-\frac{\sqrt{\beta}}{M(\xi)}\left(\frac{\rho_2}{\rho_1}+A_3\right)\mathcal{T}\left[M(\tilde{\xi})\overline{u_1}_{xt}\right]$$
$$+O\left(\alpha^2,\beta,\alpha\sqrt{\beta}\right). \quad (3.4)$$

In substituting equation (3.2) into the second equation of system (3.1), we used that

$$\left(\frac{1}{M(\xi)}\mathcal{T}\left[M(\tilde{\xi})\overline{u_1}_t\right]\right)_x=\frac{1}{M(\xi)}\mathcal{T}\left[M(\tilde{\xi})\overline{u_1}_{tx}\right]+O(\varepsilon^2), \quad (3.5)$$

with $\varepsilon^2=O(\sqrt{\beta})$. This approximation was not considered in [7], since the conformal mapping technique was not necessary along the lower flat layer. Approximation (3.5) is justified through the construction of an auxiliary PDE problem. See Appendix A for details.

The compatibility between equations (3.3) and (3.4) and the choice of a right-going wave are obtained by letting $A_1=-1$, $A_2=-\frac{1}{4}$ and $A_3=-\frac{\rho_2}{2\rho_1}$. As a result, the evolution equation for $\overline{u_1}$ can be written as

$$\overline{u_1}_t+\overline{u_1}_x+\frac{3}{2}\alpha\overline{u_1}\,\overline{u_1}_x-\frac{\rho_2}{\rho_1}\frac{\sqrt{\beta}}{2}\frac{1}{M(\xi)}\mathcal{T}\left[M(\tilde{\xi})\overline{u_1}_{xt}\right]=O\left(\beta,\alpha^2,\alpha\sqrt{\beta}\right).$$

At the interface η a similar equation can be obtained, since u_1 and η are linearly related to leading order. The equation for η can be written as

$$\eta_t+\frac{1}{M(\xi)}\eta_\xi-\frac{3}{2}\frac{\alpha}{M(\xi)}\eta\eta_\xi-\frac{\rho_2}{\rho_1}\frac{\sqrt{\beta}}{2}\frac{1}{M(\xi)}\mathcal{T}[\eta_{\xi t}]=0. \quad (3.6)$$

This is an ILW equation with variable coefficients accounting for the slowly varying bottom topography.

The constant coefficient version of equation (3.6) differs from the one deduced in [7] since the latter has a dispersion term with only spatial derivatives as in the KdV equation. The present equation reduces to a regularized dispersive model in analogy with the Benjamin-Bona-Mahony equation (BBM) [3].

For system (2.22), a similar unidirectional reduction can be obtained, leading to

$$\eta_t+\eta_x-\frac{3}{2}\alpha\eta\eta_x-\frac{\rho_2}{\rho_1}\frac{\sqrt{\beta}}{2}\mathcal{H}[\eta_{xt}]=0,$$

which is a regularized Benjamin-Ono (BO) equation over an infinite lower layer. Hence equations (3.6) is a generalization of the BO equation for intermediate depths and the presence of a topography. Recall that this equation is only valid when backscattering is negligible.

Conclusions. We derived a one-dimensional variable coefficient Boussinesq-type model for the evolution of internal waves in a two-layer system. The regime considered was a shallow upper layer and an intermediate depth lower layer. The bottom has an arbitrary, not necessarily smooth, profile generalizing the flat-bottom model derived in [7]. This arbitrary topography is dealt with by performing a conformal mapping, as in [24]. When a slowly varying topography is assumed, the model reduces to an ILW equation.

The computational implementation of the above models is relatively straightforward and will be published elsewhere together with detailed numerical experiments.

We intend to use this model to study the interaction of internal waves with different types of bottom profiles such as submerged structures and multiscale profiles. As in [23, 21], the stability analysis for the solution of the hyperbolic and weakly dispersive regimes is also of interest.

Models with a higher order pressure approximation are the objective of ongoing research and future numerical experimentation, in particular with solitary waves over a disordered topography.

Acknowledgements. The authors would like to thank Professor W. Choi for his useful comments regarding this work and future extensions.

Appendix A. Approximating the derivative of the nonlocal term. First a simple motivation: a term such as $(h(\varepsilon x)u)_x$ could be approximated as $(h(\varepsilon x)u)_x = h(\varepsilon x)u_x + O(\varepsilon)$. Nevertheless, in equations (3.5) the approximation is of higher order in ε. This is due to the fact that we can identify the Hilbert transform $\mathcal{T}\left[M(\tilde{\xi})\overline{u_1}_t\right]/M(\xi)$ with the solution of the following auxiliary problem:

$$\begin{cases} \Phi_{xx} + \Phi_{zz} = 0 & \text{on } -h_2/L + (h_2/L)h(\varepsilon x) \le z \le 0, \\ \Phi_z = \overline{u_1}_t & \text{at } z = 0, \\ \Phi_z - \varepsilon(h_2/L)h'(\varepsilon x)\Phi_x = 0 & \text{at } z = -h_2/L + (h_2/L)h(\varepsilon x), \end{cases} \tag{A.1}$$

where ε is the small parameter defined as L/l. It was already shown that through the conformal mapping procedure $\Phi_x(x,0,t) = \mathcal{T}\left[M(\tilde{\xi})\overline{u_1}_t\right]/M(\xi)$ is a relation between the horizontal velocities in both coordinate systems. Now we seek an approximation for $\Phi_{xx}(x,0,t)$, our term of interest. Keep the time variable t frozen and let $\omega(x,z) = \Phi_x(x,z,t)$. From equation (A.1), ω satisfies

$$\begin{cases} \omega_{xx} + \omega_{zz} = 0 & \text{on } -h_2/L + (h_2/L)h(\varepsilon x) \le z \le 0, \\ \omega_z = \overline{u_1}_{xt} & \text{at } z = 0, \\ \omega_z - \varepsilon(h_2/L)h'(\varepsilon x)\omega_x - \varepsilon^2(h_2/L)h''(\varepsilon x)\omega = 0 & \text{at } z = -h_2/L + (h_2/L)h(\varepsilon x). \end{cases}$$

By conformal mapping this problem is transformed into

$$\begin{cases} \omega_{\xi\xi} + \omega_{\zeta\zeta} = 0 & \text{on } -h_2/L \le \zeta \le 0, \\ \omega_\zeta = M(\xi)\overline{u_1}_{xt}\big(\mathrm{x}(\xi,0),t\big) = \overline{u_1}_{\xi t} & \text{at } \zeta = 0, \\ \omega_\zeta - \varepsilon^2(h_2/L)h''\big(\varepsilon\,\mathrm{x}(\xi,0)\big)\omega = 0 & \text{at } \zeta = -h_2/L. \end{cases}$$

Because of the Robin condition, the tangential derivative $\omega_\xi(\xi,0,t)$ is no longer $\mathcal{T}\left[M(\tilde{\xi})\overline{u_1}_{xt}\big(\mathrm{x}(\tilde{\xi},0),t\big)\right] = \mathcal{T}\left[\overline{u_1}_{\xi t}\right]$. Nevertheless, it can be approximated by this term up to a certain order in ε as follows. If we expand

$$\omega = \omega_0 + \varepsilon\omega_1 + \varepsilon^2\omega_2 + \ldots,$$

then ω_0 satisfies the Neumann problem

$$\begin{cases} \omega_{0\xi\xi} + \omega_{0\zeta\zeta} = 0 \text{ on } -h_2/L \leq \zeta \leq 0, \\ \omega_{0\zeta} = \overline{u_1}_{\xi t} \qquad \text{at } \zeta = 0, \\ \omega_{0\zeta} = 0 \qquad\quad \text{at } \zeta = -h_2/L, \end{cases}$$

with tangential derivative $\omega_{0\xi}(\xi,0) = \mathcal{T}\left[\overline{u_1}_{\xi t}\right](\xi) = \mathcal{T}\left[M(\tilde{\xi})\overline{u_1}_{xt}\big(\mathrm{x}(\tilde{\xi},0),t\big)\right](\xi)$, where $\omega_{0x} = \omega_{0\xi}/M(\xi)$. The next term is $\omega_1 = 0$, because both boundary conditions are zero. Therefore, $\omega = \omega_0 + O(\varepsilon^2)$, as established in equation (3.5).

REFERENCES

[1] W. Artiles and A. Nachbin, *Nonlinear evolution of surface gravity waves over highly variable depth*, Physical Review Letters, 93, 234501-1-234501-4, 2004.

[2] T.B. Benjamin, *Internal waves of permanent form of great depth*, Journal of Fluid Mechanics, 29, 559–592, 1967.

[3] T.B. Benjamin, J.L. Bona and J.J. Mahony, *Model equations for long waves in nonlinear dispersive systems*, Philosophical Transactions of the Royal Society of London, Series A, Math. Phys. Sci., 272(1220), 47–78, 1972.

[4] R. Camassa and C.D. Levermore, *Layer-mean quantities, local conservation laws, and vorticity*, Physical Review Letters, 78, 650–653, 1997.

[5] W. Choi and R. Camassa, *Long internal waves of finite amplitude*, Physical Review Letters, 77, 1759–1762, 1996.

[6] W. Choi and R. Camassa, *Weakly nonlinear internal waves in a two-fluid system*, Journal of Fluid Mechanics, 313, 83–103, 1996.

[7] W. Choi and R. Camassa, *Fully nonlinear internal waves in a two-fluid system*, Journal of Fluid Mechanics, 396, 1–36, 1999.

[8] R.E. Davis and A. Acrivos, *Solitary internal waves in deep water*, Journal of Fluid Mechanics, 29, 593–607, 1967.

[9] T. Driscoll, *Schwarz-Christoffel toolbox for Matlab*, http://www.math.udel.edu/driscoll/software.

[10] J.P. Fouque, J. Garnier and A. Nachbin, *Shock structure due to stochastic forcing and the time reversal of nonlinear waves*, Physica D, 195, 324–346, 2004.

[11] J.P. Fouque, J. Garnier and A. Nachbin, *Time reversal for dispersive waves in random media*, SIAM J. Appl. Math., 64(5), 1810–1838, 2004.

[12] J.P. Fouque, J. Garnier, J.C. Muñoz and A. Nachbin, *Time reversing solitary waves*, Physical Review Letters, 92, 9, 094502-1, 2004.

[13] J. Garnier and A. Nachbin, *The eddy viscosity for time reversing waves in a dissipative environment*, Physical Review Letters, 93, 15, 154501, 2004.

[14] J. Garnier and A. Nachbin, *The eddy viscosity for gravity waves propagating over turbulent surfaces*, Physics of Fluids, 18, 055101, 2006.

[15] T.C. Jo and W. Choi, *Dynamics of strongly nonlinear internal solitary waves in shallow water*, Studies in Applied Mathematics, 109, 205–227, 2002.

[16] R.I. Joseph, *Solitary waves in finite depth fluid*, J. Phys. A., 10, L225–L227, 1977.

[17] J.P. Keener, *Principles of Applied Mathematics: Transformation and Approximation*, Westview Press, 2000.

[18] T. Kubota, D. Ko and L. Dobbs, *Propagation of weakly nonlinear internal waves in a stratified fluid of finite depth*, AIAA Journal Hydrodynamics, 12, 157–165, 1978.

[19] H. Lamb, *Hydrodynamics*, Dover, 1932.

[20] Y. Matsuno, *A unified theory of nonlinear wave propagation in two-fluid systems*, Journal of the Physical Society of Japan, 62, 1902–1916, 1993.

[21] P. Milewski, E. Tabak, C. Turner, R. Rosales and F. Menzaque, *Nonlinear stability of two-layer flows*, Commun. Math. Sci., 2(3), 427–442, 2004.

[22] J.C. Muñoz and A. Nachbin, *Dispersive wave attenuation due to orographic forcing*, SIAM J. Appl. Math., 64(3), 977–1001, 2004.

[23] J.C. Muñoz and A. Nachbin, *Stiff microscale forcing and solitary wave refocusing*, SIAM Multiscale Modeling and Simulation, 3(3), 680–705, 2005.

[24] A. Nachbin, *A terrain-following Boussinesq system*, SIAM J. Appl. Math., 63, 905–922, 2003.
[25] A. Nachbin and K. Solna, *Apparent diffusion due to orographic microstructure in shallow waters*, Physics of Fluids, 15(1), 66–77, 2003.
[26] H. Ono, *Algebraic solitary waves in stratified fluids*, Journal of the Physical Society of Japan, 39, 1082–1091, 1975.
[27] T.Y. Wu, *Long waves in ocean and coastal waters*, Journal of the Engineering Mechanics Division ASCE, 107(3), 501–522, 1981.